Available online at www.sciencedirect.com
SCIENCE DIRECT
Trans. Nonferrous Met. Soc. China 17(2007) 250−256
Transactions of Nonferrous Metals Society of China
www.csu.edu.cn/ysxb/

Structural stability of intermetallic compounds of Mg-Al-Ca alloy

ZHOU Dian-wu(周惦武)[1,2], LIU Jin-shui(刘金水)[3], ZHANG Jian(张 健)[3], PENG Ping(彭 平)[3]

1. State Key Laboratory of Advanced Design and Manufacturing for Vehicle Body, Hunan University, Changsha 410082, China;
2. School of Mechanical and Automobile Engineering, Hunan University, Changsha 410082, China;
3. School of Materials Science and Engineering, Hunan University, Changsha 410082, China

Received 13 October 2006; accepted 22 December 2006

Abstract: A first-principles plane-wave pseudopotential method based on the density functional theory was used to investigate the energetic and electronic structures of intermetallic compounds of Mg-Al-Ca alloy, such as Al_2Ca, Al_4Ca and Mg_2Ca. The negative formation heat, the cohesive energies and Gibbs energies of these compounds were estimated from the electronic structure calculations, and their structural stability was also analyzed. The results show that Al_2Ca phase has the strongest alloying ability as well as the highest structural stability, next Al_4Ca, finally Mg_2Ca. After comparing the density of states of Al_2Ca, Al_4Ca and Mg_2Ca phases, it is found that the highest structural stability of Al_2Ca is attributed to an increase in the bonding electron numbers in lower energy range below Fermi level, which mainly originates from the contribution of valence electron numbers of Ca(s) and Ca(p) orbits, while the lowest structural stability of Mg_2Ca is resulted from the least bonding electron numbers near Fermi level.

Key words: plane-wave pseudopotential theory; structural stability; electronic structure; Al_2Ca; Al_4Ca; Mg_2Ca

1 Introduction

Magnesium alloys, especially approximately 90% Mg-Al-based alloys, have been used in automobile industry as cast products[1−2]. For the Mg-Al-based alloys, β-$Mg_{17}Al_{12}$ is an essential phase that plays an important role in strengthening grain boundary and suppressing high-temperature grain-boundary sliding, whereas the softening of the phase at the elevated temperature is detrimental to the creep property of the alloys. Therefore, the use of these magnesium alloys is limited. Due to the low cost, calcium has been used for improving the poor heat resistance property of Mg-Al-based alloys since 1980's, and there have been increasing attentions to the development of the Mg-Al-Ca based alloys in automobile industry as cast products.

The recent experiment investigations show that the addition of calcium to the Mg-Al-based alloys has the effect on enhancing the thermal stability of the $Mg_{17}Al_{12}$ precipitates at elevated temperatures by forming the structure of $(Mg,Ca)_{17}Al_{12}$ solid solution or has the effect on greatly improving the heat resistance by forming magnesium-calcium and aluminum-calcium intermetallic compounds[3−6]. MIN et al[7] investigated the valance electron structure(VES) of Al_2Ca，Al_4Ca and Mg_2Ca intermetallic compounds by method of the empirical electron theory(EET). They thought that the bond network of Al_2Ca has high bond energy and the difference of the bond strength between different crystalline directions is not remarkable, so its stability is the highest among the three structures studied. Both Al_4Ca and Mg_2Ca have weak bonds or weak bond zones that lead to breakage easily, which accounts for the low stability of the structure. But the alloying ability and the structural stability of these intermetallic compounds in Mg-Al-based alloys containing calcium have not been well studied yet from the alloy energy view. ZHOU et al[8] investigated the structure stability of calcium alloying $Mg_{17}Al_{12}$ phase. In this study, a first-principles plane-wave psendopotentials method based on density functional theory was used to investigate the energetic and electronic structure of Al_2Ca, Al_4Ca and Mg_2Ca phases. Moreover, the structural stability and electronic mechanism of these phases were studied.

2 Method and models of computation

2.1 Method of computation

Cambridge Serial Total Energy Package (CASTEP)

Foundation item: Project(20020530012) supported by the Doctoral Program Foundation of Ministry of Education of China
Corresponding author: ZHOU Dian-wu; Tel: +86-13017297124; E-mail: ZDWe_mail@yahoo.com.cn

[9], a first-principles plane-wave psendopotential method based on density functional theory, was used in this work. CASTEP used a plane-wave basis set for the expansion of the single-particle Kohn-Sham wave-functions, and psendopotential to describe the computationally expensive electron-ion interaction, in which the exchange-correlation energy by the generalized gradient approximation(GGA) of Perdew was adopted for all elements in the models by adopting Perdew-Burke-Ernzerhof parameters[10]. Ultrasoft psendopotential represented in reciprocal space was used[11]. A finite basis set correction and the Pulay scheme of density mixing were applied for the evaluation of energy and stress[12−14]. The atomic orbits used in the present calculations are: Mg $2p^6 3s^2$, Al $3s^2 3p^1$, Ca $3s^2 3p^6 4s^2$. To access the accuracy of computation method, a series of calculations were performed on the bulk properties of Mg, Al and Ca. The results are listed in Table 1. All atomic positions in the model were relaxed according to the total energy and force using the Broyden-Flecher-Goldfarb-Shanno(BFGS) scheme, based on the cell optimization criterion (RMs force of 5.0×10^{-5} eV/nm, stress of 0.01 GPa, and displacement of 5.0×10^{-5} nm). The calculation of total energy and electronic structure was followed by cell optimization with self-consistent-field(SCF) tolerance of 5.0×10^{-7} eV. In the present calculation, the cutoff energy of atomic wave functions (PWs), E_{cut}, was set at 330 eV. Sampling of the irreducible wedge of the Brillouin zone was performed with a regular Monkhorst-Pack grid of special *k*-points, which is 6×6×6.

2.2 Models of computation

The structure of Al_4Ca is tetragonal DI_3 type as shown in Fig.1(a). Its unit cell has the highest symmetry D_{4h}^{17}, space group I_4/mmm, 10 atoms with lattice constants of $a=b=0.435$ nm and $c=1.107$ nm. The atomic coordinates in the unit cell are

+2Ca: (0, 0, 0);

+4Al(Ⅰ): (0, 0, *z*), (0, 0, −*z*), $z=0.380$;

+4Al(Ⅱ): (0, 1/2, 1/4), (1/2, 0, 1/4).

The primitive cell of Al_4Ca was used in the calculations as shown in Fig.1(b). It has 5 atoms, i.e. 1 calcium atom and 4 aluminum atoms. 4 aluminum atoms are 2 Al(Ⅰ) and 2 Al(Ⅱ) atoms.

Al_2Ca has an ordered cubic C15 structure with lattice constants $a=b=c=0.802$ nm. As shown in Fig.1(c), its unit cell has the highest symmetry O_h^7, space group $Fd3m$. In a unit cell of the Al_2Ca phase there are 24 atoms and their atomic coordinates are as follows:

+8Ca: (0, 0, 0), (1/4, 1/4, 1/4);

+16Al: (5/8, 5/8, 5/8), (7/8, 7/8, 5/8), (5/8, 7/8, 7/8), (7/8, 5/8, 7/8).

The primitive cell of Al_2Ca was used in the calculations as shown in Fig.1(d). It has 6 atoms, i.e. 2 calcium atoms and 4 aluminum atoms.

Mg_2Ca has a hexagonal C14 type structure as shown in Fig.1(e) with the lattice constants of $a=b=0.622$ nm and $c=1.000$ nm, its unit cell has the highest symmetry D_{6h}^4, space group $P6_3/mmc$. There are 12 atoms in a unit cell and their atomic coordinates are as follows:

+4Ca: (1/3, 2/3, *z*), (−1/3, −2/3, −*z*), (1/3, 2/3, 1/2−*z*), (−1/3, −2/3, *z*−1/2), $z=0.062$;

+2Mg(Ⅰ): (0, 0, 0), (0, 0, 1/2);

+6Mg(Ⅱ): (*x*, *x*, 1/4), (−2*x*, −*x*, 1/4), (*x*, −*x*, 1/4), (−*x*, −*x*, −1/4), (2*x*, *x*, −1/4), (−*x*, *x*, −1/4), $x=-0.170$.

The unit cell of Mg_2Ca was used in the calculations.

3 Results and discussion

3.1 Equilibrium lattice constants

The lattice constants of Al_2Ca, Al_4Ca and Mg_2Ca structures were estimated from the minimized total energy. The results are listed in Table 2. It is found that the present lattice constant *a* of Al_2Ca is 0.789 nm (the value is obtained by conversion of the lattice constant 0.557 6 nm of the primitive cell of Al_2Ca), which is close to the experimental values[7] of $a=0.804$ nm and the error of lattice constant calculated here relative to the experiment result is about 1.87%. The present lattice constants *a*, *c* and *c*/*a* ratio of Al_4Ca are 0.428 nm, 1.103 nm (the value is obtained by conversion of the lattice constant 0.629 4 nm of the primitive cell of Al_4Ca), 2.58, respectively, which are close to the experimental values[16] of $a=0.436$ nm, $c=1.109$ nm and $c/a=2.54$, and the error of *c*/*a* ratio calculated here relative to the experiment result is about 1.55%. The present lattice constants *a*, *c* and *c*/*a* ratio of Mg_2Ca are 0.621 nm, 1.017 nm, 1.64, respectively, which are also close to the experimental values[7] of $a=0.624$ nm, $c=1.015$ nm and $c/a=1.67$. Hence, the computation parameters selected in this paper are suitable.

Table 1 Lattice constants and bulk modulus for Mg, Al and Ca

Element	Lattice constant/nm			Bulk modulus/GPa		
	Expt.[15]	Cal. [15]	Present	Expt.[15]	Cal. [15]	Present
Mg	0.447 7	0.445 6	0.418 6	36.9	40.5	34.1
Al	0.402 2	0.401 7	0.395 8	88.0	80.1	77.9
Ca	0.556 7	0.529 2	0.553 5	15.2	16.7	16.8

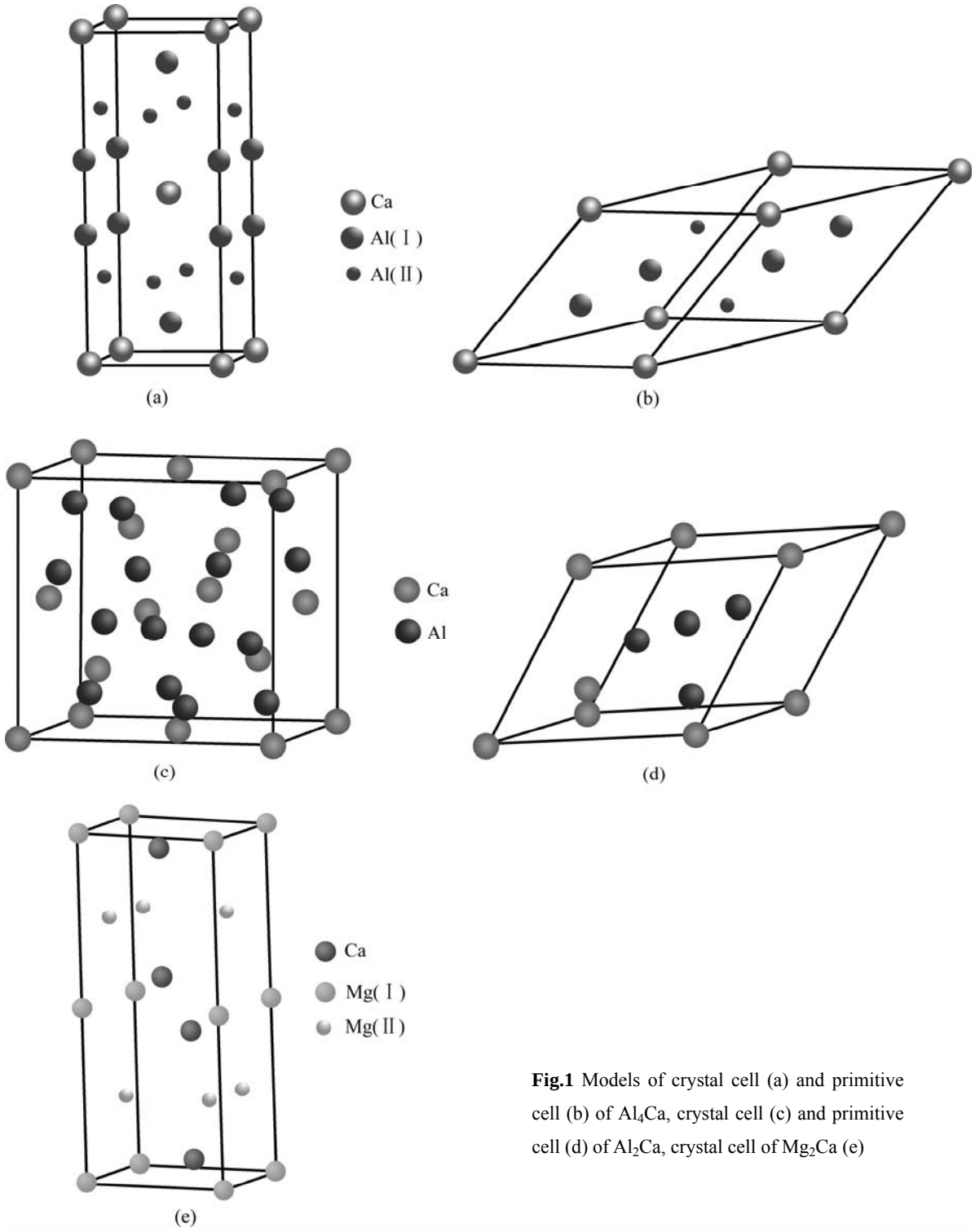

Fig.1 Models of crystal cell (a) and primitive cell (b) of Al_4Ca, crystal cell (c) and primitive cell (d) of Al_2Ca, crystal cell of Mg_2Ca (e)

Table 2 Equilibrium lattice constants (a, c), total energy (E_{tot}), formation heat (ΔH) and cohesive energy (E_{coh}) of intermetallic compounds Al_2Ca, Al_4Ca and Mg_2Ca

Compound	Lattice constant			E_{tot}/eV	ΔH/(eV·atom^{-1})	E_{coh}/(eV·atom^{-1})
	a/mm	c/mm	c/a			
Al_2Ca	0.789	−	−	−2 238.8	−0.37	−3.53
Al_4Ca	0.428	1.103	2.58	−1 233.4	−0.22	−3.52
Mg_2Ca	0.621	1.017	1.64	−1 1839.8	−0.13	−1.78

3.2 Formation heat

Formation heat (ΔH) of Al_2Ca, Al_4Ca and Mg_2Ca crystal or primitive cell per atom was calculated by using the following expression[17−18]:

$$\Delta H = E_{\text{tot}}^{\text{AB}} - [cE_{\text{form}}^{\text{A}} + (1-c)E_{\text{form}}^{\text{B}}] \quad (1)$$

where $E_{\text{tot}}^{\text{AB}}$ refers to the total energy per atom of intermetallic compound at the equilibrium lattice constant, $E_{\text{form}}^{\text{A}}$ and $E_{\text{form}}^{\text{B}}$ are the single atomic energies of pure constituents A and B in the solid states, respectively, c refers to the fractional concentration of the constituent A. The total energies of Al_2Ca, Al_4Ca primitive cell and Mg_2Ca crystal cell are also listed in Table 2. The energy of the single atom was also calculated by using the same code as crystal or primitive model. The calculated energies of Mg, Al and Ca atoms are −977.9, −57.2 and −1 003.8 eV, respectively. The calculated results of formation heat of Al_2Ca, Al_4Ca and Mg_2Ca are also listed in Table 2. It is found that formation heat of Al_2Ca and Mg_2Ca is −0.37, −0.13 eV/atom, respectively, which is close to the corresponding result of −39.1 kJ/mol (about −0.405 24 eV/atom), −4.5 kJ/mol (about −0.046 64 eV/atom), from thermodynamic data in Ref.[19]. Further analysis shows that formation heat of Al_2Ca, Al_4Ca and Mg_2Ca is all negative, which means that the structure of these phases can exist and be stable[20]. Because the negative formation heat of Al_2Ca, Al_4Ca and Mg_2Ca is increased gradually, it can be inferred that Al_2Ca phase has the strongest alloying ability, next Al_4Ca, finally Mg_2Ca.

3.3 Cohesive energy

The cohesive intensity and structural stability of crystal is correlation to its cohesive energy[20], and the cohesive energy of crystal is defined as either the energy that is needed when the crystal is formed by combining with the freedom atom, or the work that is needed when the crystal decomposes into the single atom. Hence, the bigger the cohesive energy, the more stable the crystal structure[20]. In this work, the cohesive energies (E_{coh}) of Al_2Ca, Al_4Ca and Mg_2Ca crystal or primitive cell per atom were calculated by[18]

$$E_{\text{coh}} = E_{\text{tot}}^{\text{AB}} - [cE_{\text{atom}}^{\text{A}} + (1-c)E_{\text{atom}}^{\text{B}}] \quad (2)$$

where $E_{\text{atom}}^{\text{A}}$ and $E_{\text{atom}}^{\text{B}}$ are the total energies of atoms A and B in the freedom states. The energies of Mg, Al, Ca free atom are −976.4, −53.5 and −1 001.8 eV, respectively. The energies of the free atoms were also calculated by using the same code as crystal or primitive model. The cohesive energy of the single atom of all crystal or primitive cell was calculated by Eqn.(2). The results are also listed in Table 2. It is found that the cohesive energy of the single atom of Al_2Ca is E_{coh}=−3.53 eV/atom, that of Mg_2Ca is E_{coh}=−1.78 eV/atom. Compared with the experimental results[19], the total energy of Al_2Ca is −316.9 kJ/mol (about −3.28 eV/atom), that of Mg_2Ca is −160.4 kJ/mol (about −1.66 eV/atom), the calculated results in this study are closer to the experimental values. Fig.2 shows the cohesive energies of Al_2Ca, Al_4Ca and Mg_2Ca, indicating that the cohesive energy of Al_2Ca is higher than that of Al_4Ca, and that of Mg_2Ca is only half of Al_2Ca or Al_4Ca. Hence, among the three phases, Al_2Ca phase has the highest structural stability, next Al_4Ca, finally Mg_2Ca.

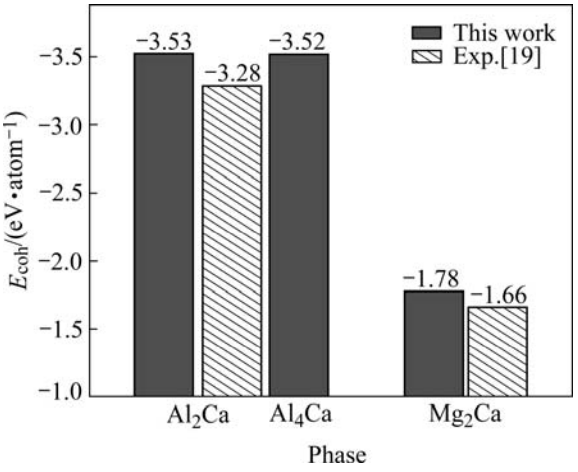

Fig.2 Cohesive energies (E_{coh}) of Al_2Ca, Al_4Ca and Mg_2Ca phases

3.4 Gibbs energy

Grounded on the above calculated results, it is found that the cohesive energy of Al_2Ca is close to that of Al_4Ca. In order to compare with the structural stability of Al_2Ca and Al_4Ca, the Gibbs energies of Al_2Ca and Al_4Ca was calculated based on some hypothetical ideas and experimental data.

Based on experiment, the relationship between Gibbs energies and temperature of Al_2Ca and Al_4Ca in the temperature range of 673−903 K can be expressed as [21]

$$\Delta G(Al_{0.67}Ca_{0.33}) = -(10.43 \pm 0.15) + (1.89 \pm 0.31) \times 10^{-3} T \quad (3)$$

$$\Delta G(Al_{0.8}Ca_{0.2}) = -(4.04 \pm 0.08) + (0.86 \pm 0.16) \times 10^{-3} T \quad (4)$$

The results calculated by Eqns.(3) and (4) are shown in Fig.3(a). It is obvious that the Gibbs energies of Al_2Ca are lower than those of Al_4Ca in the temperature range of 673−903 K. The lower the Gibbs energies are, the more stable the structure is. Hence, the

structure of Al_2Ca is more stable than that of Al_4Ca. However, the actual work temperature of intermetallic compounds of Mg-Al-Ca alloy is usually below 423 K. It is necessary to discuss the structural stability of Al_2Ca and Al_4Ca in the temperature range of 0−673 K, the results are shown in Fig.3(b).

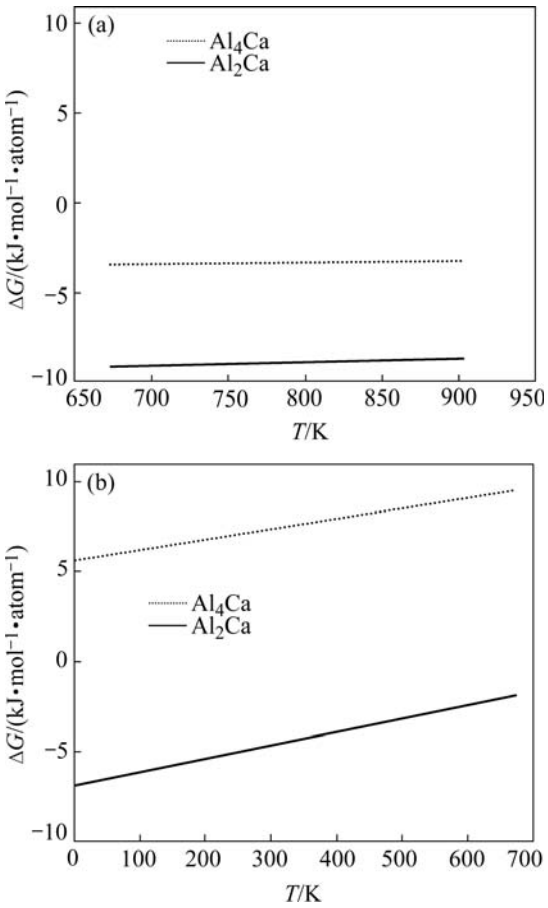

Fig.3 Relationship between Gibbs energies and temperature for Al_2Ca and Al_4Ca at different temperature ranges: (a) 673−903 K; (b) 0−673 K

Thermodynamic data from experiment measurement were summarized by OZTURK K et al[21], and the general relationship between the Gibbs energies of Al_2Ca, Al_4Ca and temperature was given by the following expression:

$$G(Al_2Ca) = 2G^{\Theta}_{fcc}(Al) + G^{\Theta}_{fcc}(Ca) - 95172 + 22.312\times10^{-3}T \quad (5)$$

$$G(Al_4Ca) = 4G^{\Theta}_{fcc}(Al) + G^{\Theta}_{fcc}(Ca) - 105347 + 29.090\times10^{-3}T \quad (6)$$

where $G^{\Theta}_{fcc}(Al)$, $G^{\Theta}_{fcc}(Ca)$ are the Gibbs energies per mole of fcc-Al, fcc-Ca, respectively.

In this work, the structural stability of Al_2Ca and Al_4Ca in the temperature range of 0−673 K was investigated by employing Eqns.(5) and (6). Here, it is necessary to replace Eqns.(5) and (6) by Eqns.(7) and (8), which can be expressed as

$$G(Al_{0.67}Ca_{0.33}) = \frac{2}{3}G^{\Theta}_{fcc}(Al) + \frac{1}{3}G^{\Theta}_{fcc}(Ca) - 31724 + 7.44\times10^{-3}T \quad (7)$$

$$G(Al_{0.8}Ca_{0.2}) = \frac{4}{5}G^{\Theta}_{fcc}(Al) + \frac{1}{5}G^{\Theta}_{fcc}(Ca) - 21069.4 + 5.82\times10^{-3}T \quad (8)$$

where $\Delta G=\Delta H-T\Delta S$ (ΔH and ΔS mean formation heat and entropy, respectively). In this work, it is supposed that there is no work exchange with environment in the systems of Al_2Ca and Al_4Ca. Moreover, there is also no change for formation heat of Al_2Ca and Al_4Ca. Hence, the following expression can be obtained based on Eqns.(7) and (8):

$$\Delta G(Al_{0.67}Ca_{0.33}) = \frac{2}{3}G^{\Theta}_{fcc}(Al) + \frac{1}{3}G^{\Theta}_{fcc}(Ca) - 31724 - G^{\Theta}(Al_{0.67}Ca_{0.33}) + 7.44\times10^{-3}T \quad (9)$$

$$\Delta G(Al_{0.8}Ca_{0.2}) = \frac{4}{5}G^{\Theta}_{fcc}(Al) + \frac{1}{5}G^{\Theta}_{fcc}(Ca) - 21069.4 - G^{\Theta}(Al_{0.8}Ca_{0.2}) + 5.82\times10^{-3}T \quad (10)$$

where $G^{\Theta}(Al_{0.67}Ca_{0.33})$, $G^{\Theta}(Al_{0.8}Ca_{0.2})$ are the Gibbs energies per mole of Al_2Ca, Al_4Ca, respectively. $G^{\Theta}_{fcc}(Al)$, $G^{\Theta}_{fcc}(Ca)$, $G^{\Theta}(Al_{0.67}Ca_{0.33})$, and $G^{\Theta}(Al_{0.8}Ca_{0.2})$ denote the total energies of fcc-Al, fcc-Ca, $Al_{0.67}Ca_{0.33}$, $Al_{0.8}Ca_{0.2}$, and their calculated values are 5.519, 96.852, −36.002, −23.801 MJ/(mol· atom), respectively. Based on these calculated data from Eqns.(9) and (10), the relationship between Gibbs energies of Al_2Ca and Al_4Ca and temperature in the range of 0−673 K can be expressed by

$$\Delta G(Al_{0.67}Ca_{0.33}) = -6.87+7.44\times10^{-3}T \quad (11)$$

$$\Delta G(Al_{0.8}Ca_{0.2}) = 5.63+5.82\times10^{-3}T \quad (12)$$

According to Eqns.(11) and (12), it is obvious that the Gibbs energies of Al_2Ca are lower than those of Al_4Ca (see Fig.3(b)), which indicates that the structure of Al_2Ca is more stable than that of Al_4Ca.

3.5 Density of states

Further analysis on the total and partial density of states(DOS) of Mg_2Ca, Al_4Ca and Al_2Ca was performed to study the electronic structure mechanism on improving structural stability. The total and partial DOSs of Al_2Ca, Al_4Ca primitive and Mg_2Ca crystal cell per atom are shown in Figs.4(a), (b) and (c), respectively. It

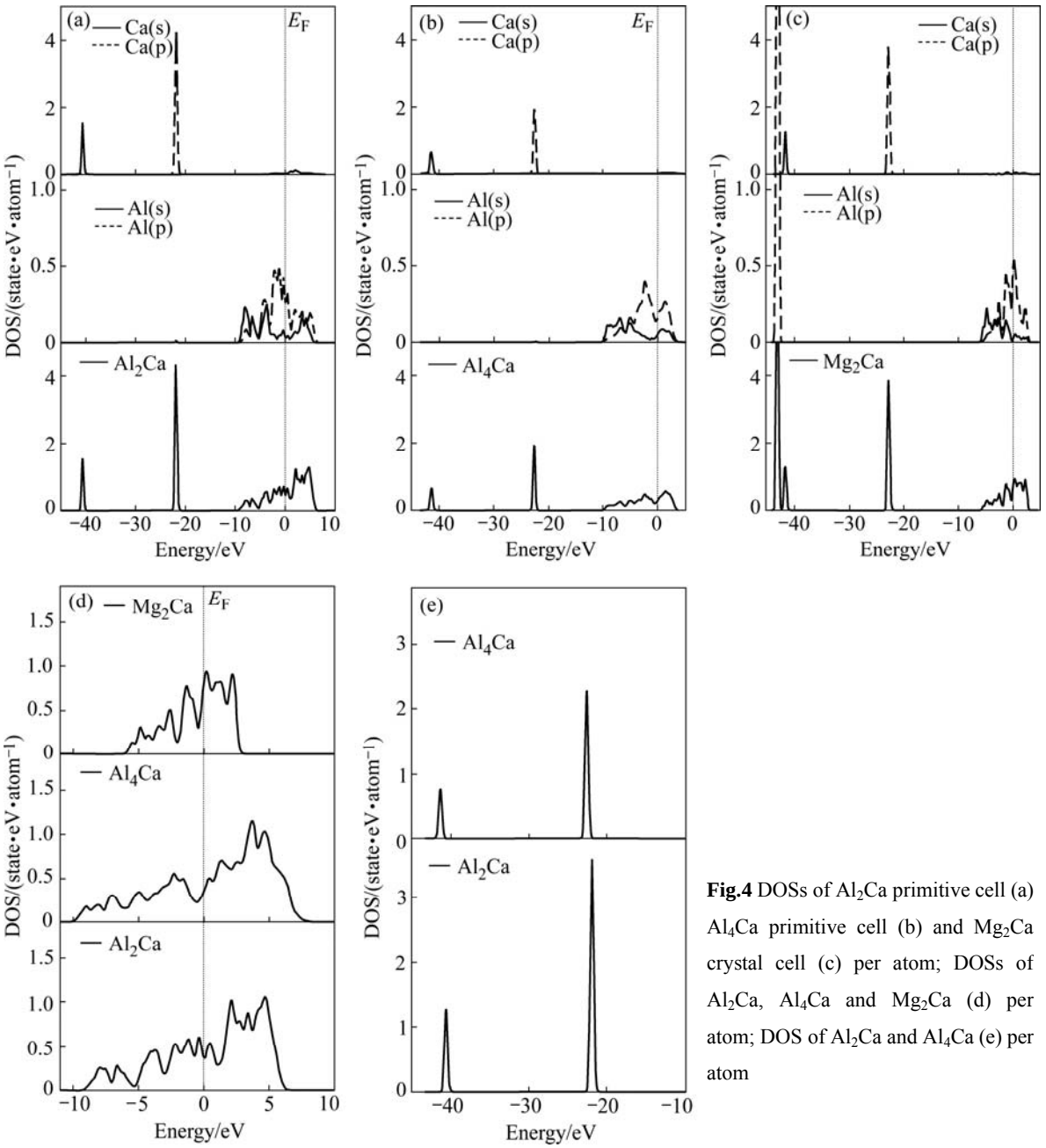

Fig.4 DOSs of Al_2Ca primitive cell (a) Al_4Ca primitive cell (b) and Mg_2Ca crystal cell (c) per atom; DOSs of Al_2Ca, Al_4Ca and Mg_2Ca (d) per atom; DOS of Al_2Ca and Al_4Ca (e) per atom

is found that the main bonding peaks between −10.0 and 10.0 eV mainly originate from the contribution of valence electron numbers of Al(s) and Al(p) orbits, while the main bonding peaks between −25 and −20 eV, −45 and −40 eV are the results of the bonding between Ca(p) and Ca(s). The energy range and the contribution of valence electron of Al_4Ca (see Fig.4(b)) are the same as those of Al_2Ca. The main bonding peaks of Mg_2Ca (see Fig.4(c)) are also located at three energy ranges, but the contribution of valence electron is different from that of Al_2Ca and Al_4Ca. The main bonding peaks between −10.0 and 10.0 eV are dominated by the valence electron numbers of Ca(p), Mg(s) and Mg(p) orbits, while the peaks between −25 and −20 eV are caused by the bonding of Ca(p), and there is a contribution of the Ca(s) and Mg(p) to two peaks between −45 and −40 eV, respectively.

The total density of states (DOS) (see Fig.4(d)) of Al_2Ca, Al_4Ca and Mg_2Ca per atom near the Fermi level were analyzed. It is found that the bonding electron numbers of Mg_2Ca are 1.981 5 between the Fermi level and −10 eV, which is smaller than 2.678 2 of Al_4Ca and 2.798 7 of Al_2Ca, respectively. The smaller the bonding electron numbers are, the weaker the charge interactions are in Refs.[22−23]. Hence, Mg_2Ca phase has the lowest structural stability. Further analysis on the density of states(DOS) (see Fig.3(e)) of primitive cell of Al_4Ca and Al_2Ca per atom was performed in low energy range far

below the Fermi level. It is found that the altitude of the main bonding peaks between −25 and −20 eV and between −45 and −40 eV is significantly different. As far as Al_4Ca is concerned, the altitude of the main bonding peaks between −25 and −20 eV is 2.241 2 electronic state/eV, the altitude between −45 and −40 eV is 0.741 2 electronic state/eV, while that of the Al_2Ca is 3.462 0 electronic state/eV, 1.240 8 electronic state/eV, respectively. This indicates that the bonding electron numbers of Al_2Ca are more than those of Al_4Ca in these two energy ranges. The more the bonding electron numbers are, the stronger the charge interactions are, and further electron numbers in low energy range far below the Fermi level will lead to more stable structure[22−23]. Hence, the structure of Al_2Ca is more stable than that of Al_4Ca.

4 Conclusions

1) The energetic and electronic structures of intermetallic compounds(Al_2Ca, Al_4Ca and Mg_2Ca) of Mg-Al-Ca alloy were investigated by using a first-principles plane-wave pseudopotential method based on the density functional theory.

2) Al_2Ca phase has the strongest alloying ability and the highest structural stability, next Al_4Ca, finally Mg_2Ca.

3) The increase of the structural stability of Al_2Ca is attributed to an increase in the bonding electron numbers at lower energy level below Fermi level, which mainly originates from the contribution of valence electron numbers of Ca(s) and Ca(p) orbits, while the lowest structural stability of Mg_2Ca is caused by the least bonding electron numbers near Fermi level.

References

[1] MORDIKE B L, EBERT T. Magnesium properties-application-potential [J]. Mater Sci Eng A, 2001, A302(1): 37−45.

[2] LUO A, PEKGULERYUZ M O. Review cast magnesium alloys for elevated temperature application [J]. J Mater Sci, 1994, 29(20): 5259−5271.

[3] MIN X G, DU W W, XIE F, SUN Y S. The melting point of $Mg_{17}Al_{12}$ phase improved by alloyed with Ca and analysis based on the empirical electron theory(EET) [J]. Chinese Sci Bull, 2002, 47(2): 109−112.

[4] SHAW C, JONES H. Structure and mechanical properties of two Mg-Al-Ca alloys consolidated from atomized power [J]. Mater Sci Tech, 1999, 15(1): 78−83.

[5] SONG H N, YUAN G Y, WANG Q D, ZHU Y P, DING W J. Microstructure and mechanical properties of heat resistant Mg-Zn-Si-Ca alloy [J]. The Chinese Journal of Nonferrous Metal, 2002, 12(5): 956−960.(in Chinese)

[6] NIE J F, MUDDLE B C. Precipitation hardening of Mg-Ca(-Zn) alloys [J]. Scripta Mater, 1997, 37(10): 1475−1481.

[7] MIN X G, SUN Y S, XUE F, DU W W, WU D Y. Analysis of valence electron structures (VES) of intermetallic compounds containing calcium in Mg-Al-based alloys [J]. Mater Chem Phys, 2002, 78(1): 88−93.

[8] ZHOU D W, PENG P, ZHUANG H L, HU Y J, LIU J S. First-principle study on structural stability of Ca alloy $Mg_{17}Al_{12}$ phase [J]. The Chinese Journal of Nonferrous Metal, 2005, 15(4): 546−551. (in Chinese)

[9] LINDAN P J D, SEGALL M D, PROBERT M J, PICKARD C J, HASNIP P J, CLARK S J, PAYNE M C. First-principles simulation: Ideas, illustrations and the CASTEP code [J]. J Phys: Condens Matter, 2002, 14(11): 2717−2744.

[10] MARLO M, MILMAN V. Density-functional study of bulk and surface properties of titanium nitride using different exchange-correlation functionals [J]. Phys Rev B, 2000, 62(4): 2899−2907.

[11] VANDERBILT D. Soft self-consistent pseudopotentitals in a generalized eigenvalue formalism [J]. Phys Rev B, 1990, 41(11): 7892−7895.

[12] HAMMER B, HANSEN L B, NORKOV J K. Improved adsorption energetics with density-functional theory using revised Perdew-Burke-Ernzerh of functionals [J]. Phys Rev B, 1999, 59(11): 7413−7421.

[13] FRANSCIS G P, PAYNE M C. Finite basis set corrections to total energy pseudopotential calcaulations [J]. J Phys: Condens Matter, 1990, 2(19): 4395−4404.

[14] MONKORST H J, PACK J D. Special points for Brillouin-zone integrations [J]. Phys Rev B, 1976, 13(12): 5188−5192.

[15] HUANG K. Solid Physics [M]. Beijing: Higher Education Press, 1985: 68.

[16] HONG S Y, FU C L. Phase stability and elastic moduli of Cr_2Nb by first-principles calculation [J]. Intermetallics, 1999, 7(1): 5−9.

[17] SAHU B R. Electronic structure and bonding of ultralight LiMg [J]. Mater Sci Eng B, 1997, B49(1): 74−78.

[18] SONG Y, GUO Z X, YANG R, LI D. First principles study of site substitution of ternary elements in NiAl [J]. Acta Mater, 2001, 49(9): 1647−1654.

[19] LI C H, HOE J L, WU P. Empirical correlation between melting temperature and cohesive energy of binary Laves phases [J]. J Phys Chem Solids, 2003, 64(2): 201−212.

[20] ZUBOV V I, TRETIAKOV N P, TEIXEIRA R J N, SANCHEZ O J F. Calculations of the thermal expansion, cohesive energy and thermodynamic stability of a van der Waals crystal-fullerene C_{60} [J]. Phys Lett A, 1995, 198(1): 223−227.

[21] OZTURK K, CHEN L Q, LIU Z K. Thermodynamic assessment of the Al-Ca binary system using random solution and associate models [J]. J Alloys Comp, 2003, 340(1/2): 199−206.

[22] FU C L, WANG X D, YE Y Y, HO K M. Phase stability, bonding mechanism, and elastic constants of Mo_5Si_3 by first-principles calculation [J]. Intermetallics, 1999, 7(2): 179−184.

[23] NYLEN J, GARCIA F J, MOSEL B D, POTTGEN R, HAUSSEVMANN U. Structural relationships, phase stability and bonding of compounds $PdSn_n$ (n=2,3,4) [J]. Solid State Sci, 2004, 6(1): 147−155.

(Edited by CHEN Wei-ping)